IT Licentiate theses
2001-014

Fourth Order Symmetric Finite Difference Schemes For The Wave Equation

ABRAHAM ZEMUI

UPPSALA UNIVERSITY
Department of Information Technology

UPPSALA UNIVERSITY

Fourth Order Symmetric Finite Difference Schemes for the Wave Equation

BY
ABRAHAM ZEMUI

December 2001

DEPARTMENT OF SCIENTIFIC COMPUTING
INFORMATION TECHNOLOGY
UPPSALA UNIVERSITY
UPPSALA
SWEDEN

Dissertation for the degree of Licentiate of Philosophy in Numerical Analysis
at Uppsala University 2001

Fourth Order Symmetric Finite Difference Schemes for the Wave Equation

Abraham Zemui
abraham@tdb.uu.se

Department of Scientific Computing
Information Technology
Uppsala University
Box 337
SE-751 05 Uppsala
Sweden

http://www.it.uu.se/

ISSN 1404-5117
Printed by the Department of Information Technology, Uppsala University, Sweden

FOURTH ORDER SYMMETRIC FINITE DIFFERENCE SCHEMES FOR THE WAVE EQUATION

ABRAHAM ZEMUI

Dec. 11, 2001

Abstract. The solution of the acoustic wave equation in one space dimension is studied. The PDE is discretized using finite element approximation. A cubic piecewise Lagrange polynomial is used as basis. Consistent finite element and lumped mass schemes are obtained. These schemes are interpreted as finite difference schemes. Error analysis is given for these finite differences (only for constant coefficients).

Key words. finite element approximation, error analysis, lumped mass approximations, finite difference approximation, Galerkin method, Helmholtz equation

1 Introduction

There are several computational methods available for solving partial differential equations which are obtained as models from different disciplines of sciences. Among these are finite differences and finite element methods. These have their own advantages and disadvantages. The success of the finite element method in elliptic problems has put pressure on numerical analysts and engineers to give up classical difference methods and adopt finite element for linear time-dependent problems. The efficiency of high-order methods has been studied by Swartz and Wendroff in [1] and by Kreiss and Oliger in [8]. On the other hand, high order finite difference operators that are used for solving partial differential equations are already obtained [2,11]. However these schemes are not symmetric whereas those obtained by finite elements are symmetric. The main goal here is to produce high order symmetric finite difference schemes. These are constructed by using finite element methods. Symmetry reduces the number of independent variables from mathematical point of view. It helps in establishing stability [12]. Thus symmetry simplifies the task of getting a numerical solution. Available software, can be applied easily for symmetric schemes. To exploit these, we first obtain finite element schemes and interpret them as finite difference schemes [3,6], thereby obtaining symmetric high order finite differences. It was observed in [7] that Galerkin's method, using a local basis, provides unconditionally stable, implicit generalized finite-difference schemes for a large class of linear and nonlinear problems. In addition Strang and Fix emphasize that finite element methods can be interpreted as finite difference methods.

Another interesting aspect is the use of lumped mass matrices. When we work with a finite element scheme, we express discrete finite element equations in terms of finite difference operators which lead to a banded matrix system. The coefficient matrix of this banded matrix system is the mass matrix. That is, the time derivative is preceded by a mass matrix which makes the time stepping implicit. To obtain an explicit scheme, one has to lump the mass matrix such that it becomes diagonal. Our construction of a finite difference scheme is based on lumping a finite element scheme with nodal basis functions which are piecewise cubic Lagrange polynomial functions and are generalizations of piecewise linear hat functions. The lumping we are using does not always produce a diagonal matrix. Some problems contain time derivatives in their boundary conditions. For such problems we have obtained a symmetric positive definite matrix as the lumped mass matrix that retains the desired order of accuracy . It should be positive definite in order for the scheme to be stable. Lumping the mass matrix can improve stability for some problems (as in our case) compared to the consistent mass matrix and make the scheme explicit. However lumping can also reduce the numerical accuracy significantly. It depends upon the equations under consideration.

In this report acoustic wave propagation in layered media is studied. The acoustic wave equation occurs in different phenomena. Acoustic waves constitute one kind of pressure fluctuation that can exist in a compressible fluid. In addition to the audible pressure fields of moderate intensity, the most familiar, there are also ultra-sonic and infra-sonic waves whose frequencies lie beyond the limits of hearing, there are also shock waves generated by explosions and supersonic aircraft and many others. When an acoustic wave traveling in one medium encounters the boundary of a second medium, reflected and transmitted waves are generated. Hence we will consider the solution of the one dimensional acoustic wave equation not only in one medium, but also in two media. There are two boundary conditions to be satisfied for all times at all points on the boundary: (1) the acoustic pressures on both sides of the boundary must be equal and (2) the normal components of the particle velocities on both sides of the boundary must be equal.

We use the finite element method (FEM) and the finite difference method (FDM) on the reduced equation, the Helmholtz equation associated with suitable boundary conditions. The purpose being to obtain efficient schemes motivated by Helmholtz equation to use for the time dependent wave propagation problems which will be applied in the sequel. The other important thing why we study the Helmholtz equation is that it makes easier to analyze accuracy. These analysis will also be applicable for the time dependent problems. Note that the stability will not be covered by studying the Helmholtz equation. For time domain stability, it is of critical importance that the mass matrix is positive definite while this is not so relevant for frequency domain problems.

In section 2, the numerical solutions of FEM in one and two media using one-sided and centered boundary approximations are described. Although boundaries are treated easily in FEM, we will have alternatives at the boundary. One-sided and centered scheme at the boundary where the latter is obtained by putting fictitious points outside the domain. This is

common in FDM. The local truncation errors for the total problem including the boundaries are presented in section 3. In section 4, FDM(schemes obtained by lumping) are discussed. In section 5, error analysis based on reflection analysis [4] is given while in section 6 numerical examples are provided, where we study the rate of convergence of the numerical methods. Finally the time dependent problem is considered in one and two media cases which is followed by concluding remarks.
The one dimensional wave equation is given by

$$\frac{1}{c^2}\frac{\partial^2 P}{\partial t^2} = \rho\frac{\partial}{\partial x}\frac{1}{\rho}\frac{\partial P}{\partial x} \tag{1.1}$$

where c = speed of sound, ρ = density and P is the acoustic pressure. Primarily, we consider the reduced wave equation, known as Helmholtz equation. The Helmholtz equation arises in many physical applications, eg. scattering problems, in electro-magnetics and acoustics. We assume the density to be constant. To get the Helmholtz equation, we assume a time harmonic dependence, then one can write the solution as

$$P(x,t) = Re(u(x)e^{-i\omega t}),\ u - complex \tag{1.2}$$

where ω = frequency. Substituting in (1.1), yields the Helmholtz equation in one dimension

$$\frac{d^2u}{dx^2} + k^2u = 0; \tag{1.3}$$

where $k = \frac{\omega}{c}$. It is to be solved in the interval $0 \leq x \leq 1$ with different boundary conditions at the end points $x = 0$ and $x = 1$. Furthermore, the equation is solved in two different media where certain boundary conditions are to be satisfied at the interface of the two media.

2 The Finite Element Method(FEM)

The idea of FEM starts by a subdivision of the structure or the region of physical interest, into smaller pieces. These pieces have to be easy to be identified by a computer and may be segments as in one space dimension or may be triangles or rectangles in two space dimensions. Then within each piece the trial functions have a simple form, usually they are polynomials. A piecewise polynomial function defined in terms of the values at nodes, defined by the element geometry, leads to a sparse coefficient matrix and the possibility of solving bigger problems. It was recognized that increasing the degree of the polynomials would greatly improve the accuracy.

In our case we have constructed the global basis as a piecewise cubic Lagrange polynomial(described below). Some other bases such as piecewise quadratic and Hermite cubic elements which are constructed by imposing continuity not only on the function but also on the first derivative have been analyzed [3]. The advantage of this approach being a reduction in the degrees of freedom. There is a double node at each point $x = jh$. Instead of being determined by the values at four distinct points, the cubic is determined by its values and its first derivatives at the two end points. This fails in the approximation of solutions which do not have a continuous derivative. There is another cubic space, formed from functions for which the second derivative is also continuous at the nodes. Such a piecewise cubic which has a continuous second derivative is called a cubic spline. It is no longer obvious which nodal parameters determine the shape of the cubic over a given subinterval, say $(j-1)h \leq x \leq jh$. The nodes x_{j-1} and x_j which belong to the interval, account for only two conditions and the other two must come from outside. Discussions on these are given in [3].
Therefore, for the FEM applied to the problem (1.3), a grid is defined by

$$\begin{aligned} x_j =& jh, \; j = 0, 1 \dots N. \\ h =& 1/N \end{aligned}$$

Let P_3^h be the space of all piecewise cubic Lagrange polynomials which are continuous at the nodes $x = jh$. We seek an approximation

$$u^h(x) = \sum_{j=0}^{N} u_j \phi_j^h(x) \tag{2.1}$$

where $u^h(x)$ is a piecewise cubic polynomial which in each interval $x_i \leq x \leq x_{i+1}$ is the Lagrange interpolating polynomial based on the nodes x_{i-1}, x_i, x_{i+1} and x_{i+2}. It implies that $u^h(x)$ is continuous at the nodes x_i but with jumps in the derivatives. Observe that the above representation involves prescribed functions $\phi_j^h(x)$ and unknown coefficients u_j. We want ϕ_j to fulfill the following:
1. ϕ_j^h is a cubic polynomial over each element, uniquely determined by its values at the nodes in the element.
2. $\phi_i^h(x_j) = \delta_{ij}$ where δ_{ij} denotes the Kronecker delta.
3. The support of $\phi_i(x_j)$ is restricted to four sub-intervals $x_{i-2} \leq x \leq x_{i+2}$
It should be noted that the u_j are just the values of the function, ie

$$u^h(x_j) = u_j$$

Moreover, any cubic polynomial defined on the whole interval can be expressed in terms of the basis namely

$$P_3(x) = \sum P_3(x_j)\phi_j^h(x)$$

which implies $P_3^h \equiv P_3(x)$

The following $\phi(x)$ constitutes a basis for integer nodes to be rescaled and translated as required. The basis functions $\phi_i^h(x)$ are then formed from $\phi(x)$ stated below in (2.3) by rescaling the independent variable from x to $\frac{x}{h}$, and translating the origin to lie at the node ih.

$$\phi_i^h(x) = \phi(\frac{x}{h} - i),\ i = 0, 1, 2 \ldots N \tag{2.2}$$

$$\phi(x) = \begin{cases} \frac{1}{6}(x+1)(x+2)(x+3),\ -2 \le x \le -1 \\ \frac{-1}{2}(x-1)(x+1)(x+2),\ -1 \le x \le 0 \\ \frac{1}{2}(x-1)(x-2)(x+1),\ 0 \le x \le 1 \\ \frac{-1}{6}(x-1)(x-2)(x-3),\ 1 \le x \le 2 \end{cases} \tag{2.3}$$

2.1 One-sided boundary approximation

Primarily we consider one-sided schemes at the boundary. The basis function need to be modified at the boundary. Accordingly, the following modifications are needed on the interval $0 \le x \le 1$ for the elements ϕ_0, ϕ_1, ϕ_2 and ϕ_3

$$\phi_0(x) = \frac{-1}{6}(x-1)(x-2)(x-3),\ 0 \le x \le 1$$

$$\phi_1(x) = \frac{1}{2}x(x-2)(x-3),\ 0 \le x \le 1$$

$$\phi_2(x) = \frac{-1}{2}x(x-1)(x-3),\ 0 \le x \le 1$$

$$\phi_3(x) = \frac{1}{6}x(x-1)(x-2),\ 0 \le x \le 1$$

Observe that the support of $\phi_3(x)$ is extended from the interval $[1, 5]$ to the interval $[0, 5]$. These modifications are equivalent to the use of one-sided

interpolation at the boundary.
We define the scalar product and the corresponding norm by

$$(u,v) = \int_0^1 \frac{1}{\rho} u(x)\overline{v}(x)dx, \;\; ||u||^2 = (u,u), \tag{2.4}$$

Now, the Galerkin method(FEM) for the Helmholtz equation is formulated as follows. Find $u^h(x)\epsilon P_3^h$ such that

$$(\frac{d^2u^h}{dx^2} + k^2u^h, v^h) = (f, v^h), \;\; v^h \epsilon P_3^h \tag{2.5}$$

f is approximated by its piecewise cubic interpolate

$$f^h = \sum_j f(x_j)\phi_j^h(x)$$

where $f(x_j)$ is the value of the function at the node $x = jh$. The treatment of the boundary conditions is straightforward. When a Dirichlet boundary condition is applied, we should require $\phi(x) = 0$ on the boundary such that the approximate solution $u^h(x)$, fulfills the boundary condition, and those boundary conditions involving derivatives can be treated by integration by parts. For instance, with a Dirichlet boundary condition at $x = 1$ and

$$\frac{du(x)}{dx} = \alpha u(x) + g, \;\; x = 0 \tag{2.6}$$

we obtain after integration by parts

$$-\sum_{j=0}^{N-1}(\int_0^1 (\phi_i^h)'(\phi_j^h)'dx)u_j - \delta_{i,0}(\alpha u_0 - g) + k^2\sum_{j=1}^{N}(\int_0^1 \phi_i^h\phi_j^h dx)u_j = \int_0^1 f^h\phi_i^h dx, \quad i = 0, \dots N-1. \tag{2.7}$$

In this case as well as the one with Dirichlet boundary conditions at both ends we obtain a linear system for $u_1, \dots, u_{N-1}$ which can be expressed in matrix form Au=b, with the matrix A having entries

$$\frac{1}{h}S_{i,j} + hk^2M_{i,j}$$

where
$S_{i,j} = -\int_0^1 \phi_i'\phi_j' dx$, $M_{i,j} = \int_0^1 \phi_i\phi_j dx$ and $b_i = \int_0^1 f^h\phi_i dx$.

The matrices S and M are called the stiffness and mass matrices respectively. It was found, for the Dirichlet boundary conditions, by computing the integrals in Maple that the stiffness matrix

$$S^D = \begin{pmatrix} \frac{-139}{45} & \frac{211}{120} & \frac{-7}{60} & \frac{-7}{360} & & & & \\ \frac{211}{120} & \frac{-118}{45} & \frac{23}{20} & \frac{1}{30} & \frac{-7}{360} & & & \\ \frac{-7}{60} & \frac{23}{20} & \frac{-32}{15} & \frac{25}{24} & \frac{1}{30} & \frac{-7}{360} & & \\ \frac{-7}{360} & \frac{1}{30} & \frac{25}{24} & \frac{-19}{9} & \frac{25}{24} & \frac{1}{30} & \frac{-7}{360} & \\ & \ddots & \ddots & \ddots & \ddots & \ddots & \ddots & \ddots & \\ & & \ddots & \ddots & \ddots & \ddots & \ddots & \ddots & \ddots \end{pmatrix}$$

and the mass matrix

$$M^D = \begin{pmatrix} \frac{1046}{945} & \frac{1}{240} & \frac{-11}{1260} & \frac{31}{15120} & & & & \\ \frac{1}{240} & \frac{223}{270} & \frac{359}{2520} & \frac{-3}{70} & \frac{31}{15120} & & & \\ \frac{-11}{1260} & \frac{359}{2520} & \frac{7}{9} & \frac{257}{1680} & \frac{-3}{70} & \frac{31}{15120} & & \\ \frac{31}{15120} & \frac{-3}{70} & \frac{257}{1680} & \frac{733}{945} & \frac{257}{1680} & \frac{-3}{70} & \frac{31}{15120} & \\ & \ddots & \ddots & \ddots & \ddots & \ddots & \ddots & \ddots & \\ & & \ddots & \ddots & \ddots & \ddots & \ddots & \ddots & \ddots \end{pmatrix}$$

With the impedance boundary condition (2.6) at $x = 0$ we obtain

$$S^I = \begin{pmatrix} \alpha + \frac{-109}{90} & \frac{22}{15} & \frac{-3}{10} & \frac{2}{45} & & & & & \\ \frac{22}{15} & \frac{-139}{45} & \frac{211}{120} & \frac{-7}{60} & \frac{-7}{360} & & & & \\ \frac{-3}{10} & \frac{211}{120} & \frac{-118}{45} & \frac{23}{20} & \frac{1}{30} & \frac{-7}{360} & & & \\ \frac{2}{45} & \frac{-7}{60} & \frac{23}{20} & \frac{-32}{15} & \frac{25}{24} & \frac{1}{30} & \frac{-7}{360} & & \\ 0 & \frac{-7}{360} & \frac{1}{30} & \frac{25}{24} & \frac{-19}{9} & \frac{25}{24} & \frac{1}{30} & \frac{-7}{360} & \\ & & \ddots & \ddots & \ddots & \ddots & \ddots & \ddots & \ddots & \\ & & & \ddots & \ddots & \ddots & \ddots & \ddots & \ddots & \ddots \end{pmatrix}$$

$$M^I = \begin{pmatrix} \frac{214}{945} & \frac{59}{315} & \frac{-31}{315} & \frac{17}{945} & & & & & \\ \frac{59}{315} & \frac{1046}{945} & \frac{1}{240} & \frac{-11}{1260} & \frac{31}{15120} & & & & \\ \frac{-31}{315} & \frac{1}{240} & \frac{223}{270} & \frac{359}{2520} & \frac{-3}{70} & \frac{31}{15120} & & & \\ \frac{17}{945} & \frac{-11}{1260} & \frac{359}{2520} & \frac{7}{9} & \frac{257}{1680} & \frac{-3}{70} & \frac{31}{15120} & & \\ 0 & \frac{31}{15120} & \frac{-3}{70} & \frac{257}{1680} & \frac{733}{945} & \frac{257}{1680} & \frac{-3}{70} & \frac{31}{15120} & \\ & & \ddots & \ddots & \ddots & \ddots & \ddots & \ddots & \ddots \\ & & & \ddots & \ddots & \ddots & \ddots & \ddots & \ddots \quad \ddots \end{pmatrix}$$

Note that when $\alpha = 0$ in (2.6), it represents Neumann boundary conditions.

Our next step was to solve the Helmholtz equation in two different media. When an acoustic wave traveling in one medium encounters the boundary of a second medium, reflected and transmitted waves are generated as in fig.1.

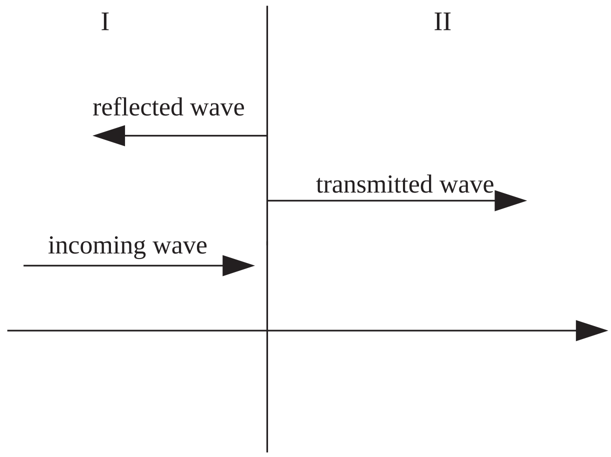

Figure 1: Reflection and transmission of a wave incident on the boundary between fluids with different characteristic impedances.

The two media could be both fluids or one of the media is a solid. The ratio of the pressure amplitudes and intensities of the reflected and transmitted waves to those of the incident wave depend on the characteristic acoustic impedances and speeds of sound in the two media and on the angle the incident wave makes with the interface. Let u_1 and u_2 be the solutions of the equation in medium 1 and 2 respectively, and let the densities and speed of sound be ρ_1, c_1 and ρ_2, c_2 in medium 1 and medium 2. The equations are to be solved in the interval $-1 \le x \le 1$. The following boundary conditions are to be satisfied at the interface of the two media, the first requiring continuity of pressure, means that there can be no net force on the plane separating the fluids. The second condition, continuity of the normal component of particle velocity, requires that the fluids remain in contact. Thus

$$u_1(0) = u_2(0) \tag{2.8}$$

$$\frac{1}{\rho_1}\frac{\partial u_1(0)}{\partial x} = \frac{1}{\rho_2}\frac{\partial u_2(0)}{\partial x} \tag{2.9}$$

The equations are

$$\rho_1 \frac{d}{dx}\left(\frac{1}{\rho_1}\frac{du_1}{dx}\right) + k_1^2 u_1 = 0, \ -1 \le x \le 0 \tag{2.10}$$

$$\rho_2 \frac{d}{dx}\left(\frac{1}{\rho_2}\frac{du_2}{dx}\right) + k_2^2 u_2 = 0, \ 0 \le x \le 1 \tag{2.11}$$

where the wave numbers are $k_1 = \frac{\omega}{c_1}$ in medium I and $k_2 = \frac{\omega}{c_2}$ in medium II. Although the waves must have the same frequency, since the speeds c_1 and c_2 are different, the wave numbers are different. The analytic solutions in the two media with an incoming wave from the left are

$$u_1(x) = e^{ik_1 x} + Re^{-ik_1 x} \tag{2.12}$$

$$u_2(x) = Te^{ik_2 x} \tag{2.13}$$

where R and T are the reflection and transmission coefficients and are given by

$$R = \frac{c_2\rho_2 - c_1\rho_1}{c_2\rho_2 + c_1\rho_1}$$

$$T = \frac{2c_2\rho_2}{c_2\rho_2 + c_1\rho_1}$$

$c_1\rho_1$ and $c_2\rho_2$ are called impedances of medium I and II respectively. To solve it numerically we apply the above concepts discussed in one medium to this problem in the interval $-1 \le x \le 1$ where u_1 is assumed to be the solution in the interval $-1 \le x \le 0$ and u_2 is the solution in the second medium $0 \le x \le 1$ and imposing equations (2.8) and (2.9) on the basis where the two media are tied. At the interface a common basis exists. The scalar product is defined by

$$\begin{aligned}(u,v) &= \int_{-1}^{1} \frac{1}{\rho} u(x)\overline{v}(x)dx \\ &= \int_{-1}^{0} \frac{1}{\rho_1} u(x)\overline{v}(x)dx + \int_{0}^{1} \frac{1}{\rho_2} u(x)\overline{v}(x)dx.\end{aligned} \tag{2.14}$$

The Galerkin formulation now leads to

$$\begin{aligned}&-\int_{-1}^{0} (\phi_i^{h_1})' \frac{1}{\rho_1} \sum_{-N_1}^{0} u_i (\phi_j^{h_1})' dx + k_1^2 \int_{-1}^{0} \phi_i^{h_1} \frac{1}{\rho_1} \sum_{-N_1}^{0} u_i \phi_j^{h_1} dx + \\ &-\int_{0}^{1} (\phi_i^{h_2})' \frac{1}{\rho_2} \sum_{0}^{N_2} u_i (\phi_j^{h_2})' dx + k_2^2 \int_{0}^{1} \phi_i^{h_2} \frac{1}{\rho_2} \sum_{0}^{N_2} u_i \phi_j^{h_2} dx = 0\end{aligned} \tag{2.15}$$

The matrices obtained are the same as in the above for the impedance boundary condition in one medium case except at the interface we have the sum of the two entries. The following is an example how the stiffness matrix looks like.

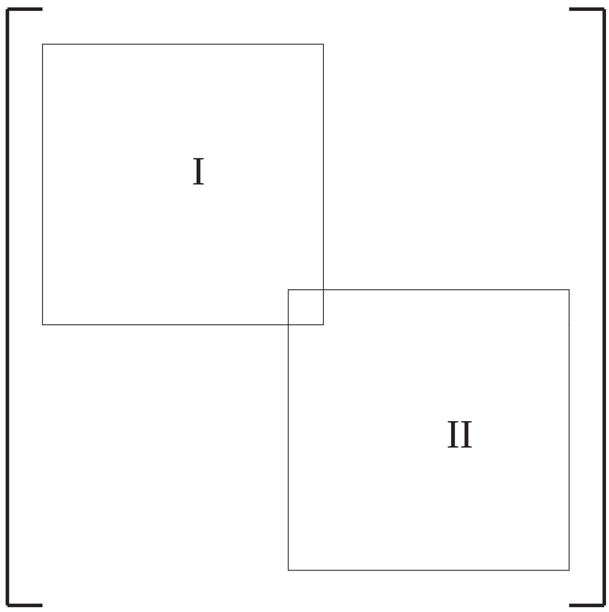

Figure 2: Stiffness matrix in two media

where

$$I = \frac{1}{h_1}\frac{1}{\rho_1}S$$

$$II = \frac{1}{h_2}\frac{1}{\rho_2}S$$

and

$$S = \begin{pmatrix}
\frac{-109}{90} & \frac{22}{15} & \frac{-3}{10} & \frac{2}{45} & & & & & & \\
\frac{22}{15} & \frac{-139}{45} & \frac{211}{120} & \frac{-7}{60} & \frac{-7}{360} & & & & & \\
\frac{-3}{10} & \frac{211}{120} & \frac{-118}{45} & \frac{23}{20} & \frac{1}{30} & \frac{-7}{360} & & & & \\
\frac{2}{45} & \frac{-7}{60} & \frac{23}{20} & \frac{-32}{15} & \frac{25}{24} & \frac{1}{30} & \frac{-7}{360} & & & \\
\frac{-7}{360} & \frac{1}{30} & \frac{25}{24} & \frac{-19}{9} & \frac{25}{24} & \frac{1}{30} & \frac{-7}{360} & & & \\
 & \ddots & \ddots & \ddots & \ddots & \ddots & \ddots & \ddots & & \\
 & & \frac{-7}{360} & \frac{1}{30} & \frac{25}{24} & \frac{-19}{9} & \frac{25}{24} & \frac{1}{30} & \frac{-7}{360} & \\
 & & & \frac{-7}{360} & \frac{1}{30} & \frac{25}{24} & \frac{-32}{15} & \frac{23}{20} & \frac{-7}{60} & \frac{2}{45} \\
 & & & & \frac{-7}{360} & \frac{1}{30} & \frac{23}{20} & \frac{-118}{45} & \frac{211}{120} & \frac{-3}{10} \\
 & & & & & \frac{-7}{360} & \frac{-7}{60} & \frac{211}{120} & \frac{-139}{45} & \frac{22}{15} \\
 & & & & & & \frac{2}{45} & \frac{-3}{10} & \frac{22}{15} & \frac{-109}{90}
\end{pmatrix}$$

Moreover, at the interface where the two block matrices overlap, the entry for the stiffness matrix is

$$\frac{1}{h_1}\frac{1}{\rho_1}\frac{-109}{90} + \frac{1}{h_2}\frac{1}{\rho_2}\frac{-109}{90}$$

where h_1 and h_2 are the step sizes in the respective media. The same applies for the mass matrix.

2.2 Centered boundary approximations

We have also implemented a centered scheme at the boundary for comparison with one sided schemes. Here the support is extended to the left, ie., we consider the grid points x_{-1}, x_0, x_1, x_2, etc as shown below such that $x = 0$ which is not necessarily a grid point lies between x_0 and x_1 and $x_0 = -\alpha h$ where h is the step size and $0 \leq \alpha \leq 0.5$. We refrain from taking $0.5 < \alpha < 1$ as it produces a singularity for $\alpha = 1$, and for some values it is almost one sided. If the latter case arises we will use only the points x_0 x_1 and x_2 . It should be noted that the main reason why we put $\alpha \neq 0$

into consideration is that in two-dimensional irregular domains we cannot expect $\alpha = 0$.

Figure 3: Arrangements of grid points for the centered scheme at the boundary.

Now considering the Dirichlet boundary condition, we have added $\phi_{-1}(x)$ for the basis defined in (2.3) and modified $\phi_{-1}(x)$, $\phi_1(x)$ and $\phi_2(x)$ to satisfy the essential boundary condition.

$$\phi_{-1}(new) = \phi_{-1}(x) - \frac{\phi_{-1}(\alpha)}{\phi_0(\alpha)}\phi_0(x)$$
$$\phi_1(new) = \phi_1(x) - \frac{\phi_1(\alpha)}{\phi_0(\alpha)}\phi_0(x)$$
$$\phi_2(new) = \phi_2(x) - \frac{\phi_2(\alpha)}{\phi_0(\alpha)}\phi_0(x)$$

For the Neumann boundary condition no changes have been made. However for the two media case we keep the right and left sides and modify ϕ_0 in order the continuity conditions to be fulfilled at the interface as

$$\phi_0 = \begin{cases} \frac{\phi_0^l(x)}{\phi_0^l(\alpha)}, & x \le 0 \\ \frac{\phi_0^r(x)}{\phi_0^r(\alpha)}, & x \ge 0 \end{cases}$$

Consequently for $\alpha = 0$, the following stiffness and mass matrices are obtained, respectively for the Dirichlet boundary condition.

$$S^D = \begin{pmatrix} \frac{-1}{45} & \frac{1}{60} & \frac{-7}{360} & & & & & & & \\ \frac{1}{60} & \frac{-94}{45} & \frac{25}{24} & \frac{1}{30} & \frac{-7}{360} & & & & & \\ \frac{-7}{360} & \frac{25}{24} & \frac{-19}{9} & \frac{25}{24} & \frac{1}{30} & \frac{-7}{360} & & & & \\ 0 & \frac{1}{30} & \frac{25}{24} & \frac{-19}{9} & \frac{25}{24} & \frac{1}{30} & \frac{-7}{360} & & & \\ 0 & \frac{-7}{360} & \frac{1}{30} & \frac{25}{24} & \frac{-19}{9} & \frac{25}{24} & \frac{1}{30} & \frac{-7}{360} & & \\ & & \ddots & \ddots & \ddots & \ddots & \ddots & \ddots & \ddots & \\ & & & \ddots & \ddots & \ddots & \ddots & \ddots & \ddots & \ddots \end{pmatrix}$$

$$M^D = \begin{pmatrix} \frac{2}{945} & \frac{-3}{140} & \frac{31}{15120} & & & & & & \\ \frac{-3}{140} & \frac{731}{945} & \frac{257}{1680} & \frac{-3}{70} & \frac{31}{15120} & & & & \\ \frac{31}{15120} & \frac{257}{1680} & \frac{733}{945} & \frac{257}{1680} & \frac{-3}{70} & \frac{31}{15120} & & & \\ 0 & \frac{-3}{70} & \frac{257}{1680} & \frac{733}{945} & \frac{257}{1680} & \frac{-3}{70} & \frac{31}{15120} & & \\ 0 & \frac{31}{15120} & \frac{-3}{70} & \frac{257}{1680} & \frac{733}{945} & \frac{257}{1680} & \frac{-3}{70} & \frac{31}{15120} & \\ & & \ddots & \ddots & \ddots & \ddots & \ddots & \ddots & \ddots \\ & & & \ddots & \ddots & \ddots & \ddots & \ddots & \ddots \quad \ddots \end{pmatrix}$$

One can imagine easily how the corresponding matrices for impedance and for the two media cases looks like. Hence we avoid listing them.

3 Local truncation errors

Error estimates for FEM based on Galerkin methods are determined by the approximation property of the finite element space. In other words if V_h is a space of piecewise polynomials of degree $r-1$, from approximation theory we know that there is a v_h in V_h such that

$$||v - v_h|| \leq const \, . \, h^r$$

for v smooth enough, $v \epsilon V_h$. Then there is an error estimate for the solution u_h such that

$$||u - u_h|| \leq const \, . \, h^r$$

In the subsequent discussions we use the conventional error analysis of FDM. We first consider the standard rows for the interior points far from the boundaries of the stiffness and mass matrices which are respectively

$$\frac{1}{h}(\frac{-7}{360} \; \frac{1}{30} \; \frac{25}{24} \; \frac{-19}{9} \; \frac{25}{24} \, \frac{1}{30} \, \frac{-7}{360})$$

and

$$h(\frac{31}{15120} \; \frac{-3}{70} \; \frac{257}{1680} \; \frac{733}{945} \; \frac{257}{1680} \; \frac{-3}{70} \; \frac{31}{15120})$$

The Galerkin method can be viewed as a difference method for u_j. Exploitation of this point of view led to the super-convergence results of [6] and [10] which we apply for our scheme

$$hk^2(\frac{31}{15120}u_{j-3} - \frac{3}{70}u_{j-2} + \frac{257}{1680}u_{j-1} + \frac{733}{945}u_j + \frac{257}{1680}u_{j+1} - \frac{3}{70}u_{j+2} + \frac{31}{15120}u_{j+3}) \\ + \frac{1}{h}(\frac{-7}{360}u_{j-3} + \frac{1}{30}u_{j-2} + \frac{25}{24}u_{j-1} - \frac{19}{9}u_j + \frac{25}{24}u_{j+1} + \frac{1}{30}u_{j+2} - \frac{7}{360}u_{j+3}) = 0 \tag{3.1}$$

Correspondingly, it was found that the local truncation error by Taylor series is

$$hu''(x_i) - \frac{11}{360}h^5u^{(6)} - \frac{59}{10080}h^7u^{(8)}$$

and

$$hu(x_i) - \frac{11}{360}h^5u^{(4)} - \frac{23}{7560}h^7u^{(6)}$$

Observe here that super-convergence is attained, ie., the stiffness matrix is a $4th$ order approximation of $\frac{d^2}{dx^2}$ whereas (3.1) is a $6th$ order accurate approximation of

$$u'' + k^2u = 0$$

In addition to the interior points we have also tried to determine the accuracy of the interior including the boundaries. We have listed tables of Taylor series expansions for the different boundary conditions encountered.

row	stiffness
1	$\frac{31}{24}hu_0'' + \frac{79}{72}h^2u_0''' + \frac{637}{1440}h^3u_0^{(4)} + \frac{59}{1440}h^4u_0^{(5)} + \ldots$
2	$\frac{5}{6}hu_0'' + \frac{173}{90}h^2u_0''' + \frac{37}{18}h^3u_0^{(4)} + \frac{64}{75}h^4u_0^{(5)} \ldots$
3	$\frac{25}{24}hu_0'' + \frac{1087}{360}h^2u_0''' + \frac{6467}{1440}h^3u_0^{(4)} + \frac{1291}{288}h^4u_0^{(5)} \ldots$

Table 1: Taylor series expansion for the first three non-regular rows of the stiffness matrix with a Dirichlet boundary condition.

row	mass
1	$\frac{79}{72}h^2u_0' + \frac{97}{180}h^3u_0'' + \frac{29}{168}h^4u_0''' \ldots$
2	$\frac{173}{90}h^2u_0' + \frac{89}{45}h^3u_0'' + \frac{93}{70}h^4u_0''' \ldots$
3	$\frac{1087}{360}h^2u_0' + \frac{811}{180}h^3u_0'' + \frac{3781}{840}h^4u_0''' \ldots$

Table 2: Taylor series expansion for the first three non-regular rows of the mass matrix with a Dirichlet boundary condition.

Although the truncation error is large at the boundary, still the scheme is of order 5 for FEM (to be proved in section(5)) and of order 4 for FDM. The local truncation error is of order three. To justify our claim for the local truncation error we have divided the FEM scheme by h to have analogy with finite difference techniques. From the tables (1) and (2) and from the differential equation(1.3), since $u(0) = 0$ from the boundary condition the even order derivatives vanish, and $u'''(0) = k^2u'(0)$ is used in each row. Then we are left with h^3 in both tables as truncation error. Therefore we infer that FEM is of order three at the boundary. It is proved in [9] that for certain classes of difference schemes it is possible to lower the accuracy one order at the boundary without losing the convergence rate defined by the interior scheme. However here it turns out that the global error is of order 5 while the local truncation error at the boundary is of order 3.

For the sake of completeness we list below the Taylor series expansions of the stiffness and mass matrices for the Neumann boundary conditions. The local truncation error at the boundary is of order 2 and the global error is of order four for both FEM and FDM.

row	stiffness
1	$\frac{-1}{3}hu_0'' + \frac{2}{45}h^2u_0''' + \frac{1}{90}h^3u_0^{(4)} + \frac{1}{45}h^4u_0^{(5)} \dots$
2	$\frac{31}{24}hu_0'' + \frac{79}{72}h^2u_0''' + \frac{637}{1440}h^3u_0^{(4)} + \frac{59}{1440}h^4u_0^{(5)} \dots$
3	$\frac{5}{6}hu_0'' + \frac{173}{90}h^2u_0''' + \frac{37}{18}h^3u_0^{(4)} + \frac{64}{45}h^4u_0^{(5)} \dots$
4	$\frac{25}{24}hu_0'' + \frac{1087}{360}h^2u_0''' + \frac{6467}{1440}h^3u_0^{(4)} + \frac{1291}{288}h^4u_0^{(5)} \dots$

Table 3: Taylor series expansion for the first four non-regular rows of the stiffness matrix where Neumann boundary conditions is employed.

row	mass
1	$\frac{1}{3}h^2u_0 + \frac{-1}{45}h^3u_0'' + \frac{-2}{105}h^4u_0''' \dots$
2	$\frac{31}{24}h^2u_0 + \frac{91}{180}h^3u_0'' + \frac{139}{840}h^4u_0''' \dots$
3	$\frac{5}{6}h^2u_0 + \frac{89}{45}h^3u_0'' + \frac{93}{70}h^4u_0''' \dots$
4	$\frac{25}{24}h^2u_0 + \frac{811}{180}h^3u_0'' + \frac{3781}{840}h^4u_0''' \dots$

Table 4: Taylor series expansion for the first non-regular rows of the mass matrix where Neumann boundary condition is employed.

In a similar fashion we reach the same conclusion for the centered scheme at the boundary.

row	stiffness
1	$\frac{-1}{24}hu_0'' + \frac{-7}{360}h^2u_0''' + \frac{-19}{1440}h^3u_0^{(4)} + \frac{-7}{1440}h^4u_0^{(5)} \dots$
2	$\frac{25}{24}hu_0'' + \frac{353}{360}h^2u_0''' + \frac{739}{1440}h^3u_0^{(4)} + \frac{233}{1440}h^4u_0^{(5)} \dots$
3	$hu_0'' + 2h^2u_0''' + 2h^3u_0^{(4)} + \frac{4}{3}h^4u_0^{(5)} \dots$
4	$hu_0'' + 3h^2u_0''' + \frac{9}{2}h^3u_0^{(4)} + \frac{9}{2}h^4u_0^{(5)} \dots$

Table 5: Taylor series expansion for the first four non-regular rows of the stiffness matrix of the centered scheme at the boundary with Dirichlet boundary condition.

It is of order four, but the centered scheme is better as we compare the constant terms in the respective truncation errors.

row	mass
1	$\frac{-7}{360}h^2u_0' + \frac{-1}{180}h^3u_0'' + \frac{-1}{840}h^4u_0''' \dots$
2	$\frac{353}{360}h^2u_0' + \frac{91}{180}h^3u_0'' + \frac{139}{840}h^4u_0''' \dots$
3	$2h^2u_0' + 2h^3u_0'' + \frac{4}{3}h^4u_0''' \dots$
4	$3h^2u_0' + \frac{5639}{1260}h^3u_0'' + \frac{9}{2}h^4u_0''' \dots$

Table 6: Taylor series expansion for the first non-regular rows of the mass matrix of the centered scheme at the boundary with Dirichlet boundary condition.

4 Lumped Mass Matrix

To obtain an explicit scheme in the time dependent problem, it is common to lump the mass matrix such that it becomes diagonal. It should be noted that the stiffness matrix is retained as in FEM. We have lumped the mass matrix as follows. For a regular row, ie., one corresponding to an interior point away from the boundary, we simply lump the mass matrix to a single diagonal entry equal to 1. It is evident from the local truncation error obtained on page (14) that this approximation will keep fourth order accuracy although the super-convergence of the FEM scheme is lost. For the non-regular rows which are affected by the boundary conditions we consider the Taylor series expansion of each and we seek fourth order accuracy by making the mass matrix diagonal, if it is possible, otherwise by making the mass matrix symmetric and positive definite. The latter happens when we consider two different media. In the subsequent we give examples of the steps performed in obtaining the entries for the non -regular rows of the lumped matrix for different boundary conditions. To begin with, consider Dirichlet boundary conditions and let us look the Taylor series expansions given in tables 7 and 8.

row	stiffness
1	$\frac{31}{24}hu_0'' + \frac{79}{72}h^2u_0''' + \frac{637}{1440}h^3u_0^{(4)} + \frac{59}{1440}h^4u_0^{(5)} + \dots$
2	$\frac{5}{6}hu_0'' + \frac{173}{90}h^2u_0''' + \frac{37}{18}h^3u_0^{(4)} + \frac{64}{75}h^4u_0^{(5)} \dots$
3	$\frac{25}{24}hu_0'' + \frac{1087}{360}h^2u_0''' + \frac{6467}{1440}h^3u_0^{(4)} + \frac{1291}{288}h^4u_0^{(5)} \dots$

Table 7: Taylor series expansion for the first three non-regular rows of the stiffness matrix.

row	mass	lumped(FD)
1	$\frac{79}{72}h^2u_0' + \frac{97}{180}h^3u_0'' + \frac{29}{168}h^4u_0''' \dots$	$\frac{79}{72}$
2	$\frac{173}{90}h^2u_0' + \frac{89}{45}h^3u_0'' + \frac{93}{70}h^4u_0''' \dots$	$\frac{173}{90}$
3	$\frac{1087}{360}h^2u_0' + \frac{811}{180}h^3u_0'' + \frac{3781}{840}h^4u_0''' \dots$	$\frac{1087}{360}$

Table 8: Taylor series expansion for the first three non-regular rows of the mass matrix including the entries in the lumped mass matrix.

It should be noted that using the differential equation (1.3) and the boundary conditions, the derivatives of the second order in the Taylor series expansions in both tables vanish. Moreover the derivatives of order three in the Taylor series expansion of the stiffness matrix cancels its corresponding derivatives of first order in the Taylor series expansion of the mass matrix. Now we want the diagonal elements in the lumped scheme to be the coefficients that occur in the cancellations, and use

$$\gamma u_i = \xi(u_0 + ihu_0' + \frac{(ih)^2}{2}u_0'' + \dots)$$

letting γ to be the principal coefficients that occurred in the cancellations and ξ to be the diagonal elements in the lumped mass matrix.
From this equation we determine the value of ξ which is the value of one of the diagonals as they are given in the above table and the following matrix.

$$M^l = \begin{pmatrix} \frac{79}{72} & & & & & \\ & \frac{173}{180} & & & & \\ & & \frac{1087}{1080} & & & \\ & & & 1 & & \\ & & & & \ddots & \\ & & & & & \ddots \end{pmatrix}$$

Applying the same technique for the Neumann boundary condition, the lumped mass matrix is found to be

$$M^{lN} = \begin{pmatrix} \frac{1}{3} & & & & & & \\ & \frac{31}{24} & & & & & \\ & & \frac{5}{6} & & & & \\ & & & \frac{25}{24} & & & \\ & & & & 1 & & \\ & & & & & \ddots & \\ & & & & & & \ddots \end{pmatrix}$$

However in lumping the mass matrix, for the third boundary condition(impedance) we considered, the change is significant as it is no longer restricted to the first row as in FEM. Suppose one uses the following boundary condition

$$\frac{du(0)}{dx} - \alpha u(0) = 0, \tag{4.1}$$

As in the above the Taylor series expansion of each row is found.

row	stiffness
1	$\alpha u_0 + u_0' + \frac{1}{3}hu_0'' + \frac{2}{45}h^2u_0''' + \frac{1}{90}h^3u_0^{(4)} + \dots$
2	$\frac{31}{24}hu_0'' + \frac{79}{72}h^2u_0''' + \frac{637}{1440}h^3u_0^{(4)} + \dots$
3	$\frac{5}{6}hu_0'' + \frac{173}{90}h^2u_0''' + \frac{37}{18}h^3u_0^{(4)} + \dots$
4	$\frac{25}{24}hu_0'' + \frac{1087}{360}h^2u_0''' + \frac{6467}{1440}h^3u_0^{(4)} + \dots$

Table 9: Taylor series expansion for the first four non regular rows of the stiffness matrix of the impedance boundary condition.

row	mass	lumped(FD)
1	$\frac{1}{3}hu_0 + \frac{2}{45}h^2u_0' - \frac{1}{45}h^3u_0'' + \ldots$	$\frac{1}{3} - \frac{2}{45}\alpha h$
2	$\frac{31}{24}hu_0 + \frac{79}{72}h^2u_0' + \frac{97}{180}h^3u_0'' + \ldots$	$\frac{31}{24} + \frac{14}{72}\alpha h$
3	$\frac{5}{6}hu_0 + \frac{173}{90}h^2u_0' + \frac{89}{45}h^3u_0'' + \ldots$	$\frac{5}{6} - \frac{23}{90}\alpha h$
4	$\frac{25}{24}hu_0 + \frac{1087}{360}h^2u_0' + \frac{811}{180}h^3u_0'' + \ldots$	$\frac{25}{24} + \frac{38}{60}\alpha h$

Table 10: Taylor series expansion for the first four non regular rows of the mass matrix of the impedance boundary condition.

We observe that the principal coefficients in both expansions cancel each other, namely the coefficients of the derivatives of the second order in the Taylor series expansion of the stiffness matrix with that of the undifferentiated function in the Taylor series expansion of the mass matrix . Besides the coefficients of the derivatives of order three in the Taylor series expansion of the stiffness matrix cancel out those coefficients of the first order derivatives in the Taylor series expansion of the mass matrix. Consequently, to find the entries in the lumped mass matrix of this, where the impedance boundary condition is applied, we use

$$\gamma u_i + \rho u_i' = \xi(u_0 + ihu_0' + \frac{(ih)^2}{2}u_0'' + \ldots) + \beta u_i'$$

and the boundary condition $u_0' = \alpha u_0$, where γ,ρ represents the coefficients of the principal and those of the first order derivative that occurred in the cancellation described above and ξ and β are to be determined for each row. Consequently, the lumped mass matrix turns out to be

$$M^{lI} = \begin{pmatrix} \frac{1}{3} - \frac{2}{45}\alpha h & & & & & & \\ & \frac{31}{24} + \frac{14}{72}\alpha h & & & & & \\ & & \frac{5}{6} - \frac{23}{90}\alpha h & & & & \\ & & & \frac{25}{24} + \frac{38}{60}\alpha h & & & \\ & & & & 1 & & \\ & & & & & \ddots & \\ & & & & & & \ddots \end{pmatrix}$$

The above matrix is positive definite for sufficiently small αh. Before we proceed, it is worth mentioning that the above procedure of lumping does not work when we have inflow boundary condition such as

$$\frac{\partial u}{\partial x} + \frac{\partial u}{\partial t} = f \tag{4.2}$$

Hence we have formed non-diagonal lumping which is symmetric and positive definite. Positive definiteness should be guaranteed in order for the time dependent equations to be stable. To prove our claim, we consider the discrete form of the wave equation.
We introduce a grid in time, with points $t_n = n\triangle t$, $n = 0, 1, 2, \dots$
A time discrete function u^n can then be defined. We approximate the time derivative by a centered second order accurate finite difference formula

$$\frac{\partial^2}{\partial t^2} = \frac{u^{n+1} - 2u^n + u^{n-1}}{(\triangle t)^2} \tag{4.3}$$

The discrete form is

$$M\frac{u^{n+1} - 2u^n + u^{n-1}}{(\triangle t)^2} - Su^n = 0 \tag{4.4}$$

where M and S are mass and stiffness matrices respectively, and it is equivalent to

$$u^{n+1} - (2 + (\triangle t)^2 M^{-1}S)u^n + u^{n-1} = 0 \tag{4.5}$$

We shall assume that the eigenvalues of S are non-positive, which is the case with Dirichlet or Neumann boundary conditions. Then the eigenvalues λ of $M^{-1}S$ are also non-positive by the identity

$$x^*Sx = \lambda x^*Mx$$

provided that M is positive definite. By a change of coordinates $v = M^{1/2}u$, the matrix $M^{-1}S$ goes over into the symmetric matrix $M^{-1/2}SM^{-1/2}$ and the difference equation (4.5) becomes equivalent to a set of scalar equations

$$v^{n+1} - (2 + \triangle t\lambda)v^n + v^{n-1} = 0 \tag{4.6}$$

with $\lambda \leq 0$. This equation is stable if

$$\triangle t \leq 2\,|\lambda|^{-1/2}$$

Therefore the stability limit on $\triangle t$ is determined by the largest eigenvalues of $-M^{-1}S$.
We now going to construct a symmetric and positive definite lumped mass matrix. It suffices to consider the non-regular rows. Since there are four rows of these, we form the following system of equations

$$\sum_{j=1}^{4} m_{i,j}u_{j-1} = \xi_i u_0 + \beta_i h u_0', \; i = 1, 2, 3, 4 \tag{4.7}$$

where ξ_i and β_i are the coefficients of u_0 and u_0' respectively in the ith row for the Taylor series expansion of the mass matrix shown in table(8). Applying Taylor series expansion for the left hand side of the equation and requiring symmetry, a system of 8 equations and 10 unknowns is solved, ie., we have three free parameters. The following entries were obtained.

$$\begin{pmatrix} \frac{142}{45}+t_2-4t_3+4t_1 & \frac{-256}{45}-2t_2+8t_3-7t_1 & \frac{43}{15}+t_2-4t_3+2t_1 & t_1 \\ \frac{-256}{45}-2t_2+8t_3-7t_1 & \frac{2147}{180}+4t_2-15t_3+12t_1 & \frac{-361}{90}-2t_2+6t_3-3t_1 & \frac{-337}{360}+t_3-2t_1 \\ \frac{43}{15}+t_2-4t_3+2t_1 & \frac{-361}{90}-2t_2+6t_3-3t_1 & t_2 & \frac{89}{45}-2t_3+t_1 \\ t_1 & \frac{-337}{360}+t_3-2t_1 & \frac{89}{45}-2t_3+t_1 & t_3 \end{pmatrix}$$

At this stage we require the above matrix (the lumped mass matrix) to be positive definite. As an example for $\triangle t$ small enough, it was found by inspection $t_1 = 1$, $t_2 = 2$ and $t_3 = 1$ produce the required order of accuracy and stable scheme.

$$\begin{pmatrix} \frac{232}{45} & \frac{-391}{45} & \frac{43}{15} & 1 \\ \frac{-391}{45} & \frac{3047}{180} & \frac{-451}{90} & \frac{-697}{360} \\ \frac{43}{15} & \frac{-451}{90} & 2 & \frac{44}{45} \\ 1 & \frac{-697}{360} & \frac{44}{45} & 1 \end{pmatrix}$$

Finally for the two media case, the lumped matrix is not diagonal throughout. It is to be recalled that in constructing the lumped mass matrix, we require the mass matrix to attain fourth order accuracy which is established by Taylor series expansion and also imposing the boundary conditions. However, at the interface there are only continuity conditions. Hence at the interface, it is the positive definite matrix shown above. In general the matrix is as in fig.4.

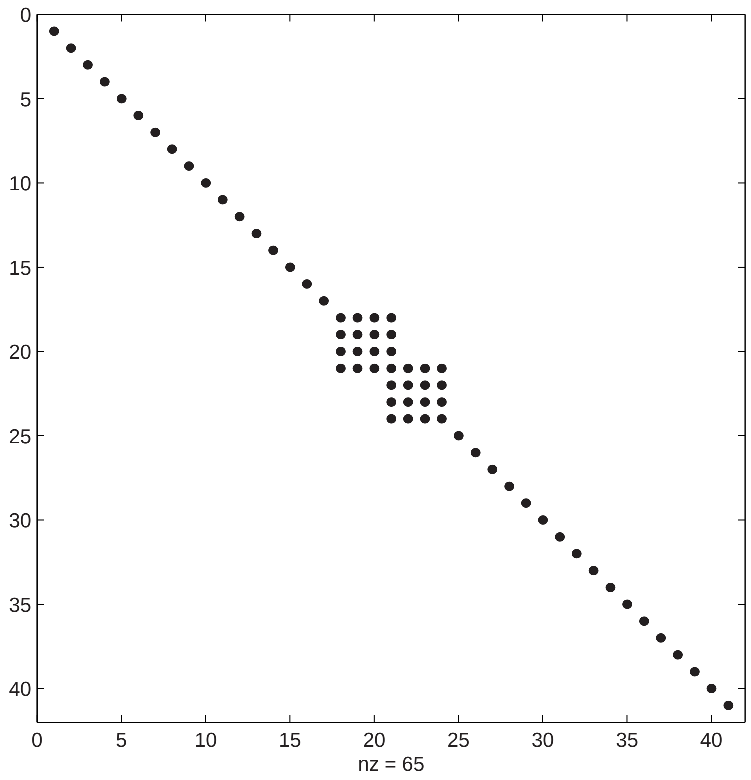

Figure 4: Lumped mass matrix which is symmetric positive definite at the interface.

Furthermore the lumped mass matrix for the wave equation in the two media case with the impedance boundary condition given in (4.2), has the following form.

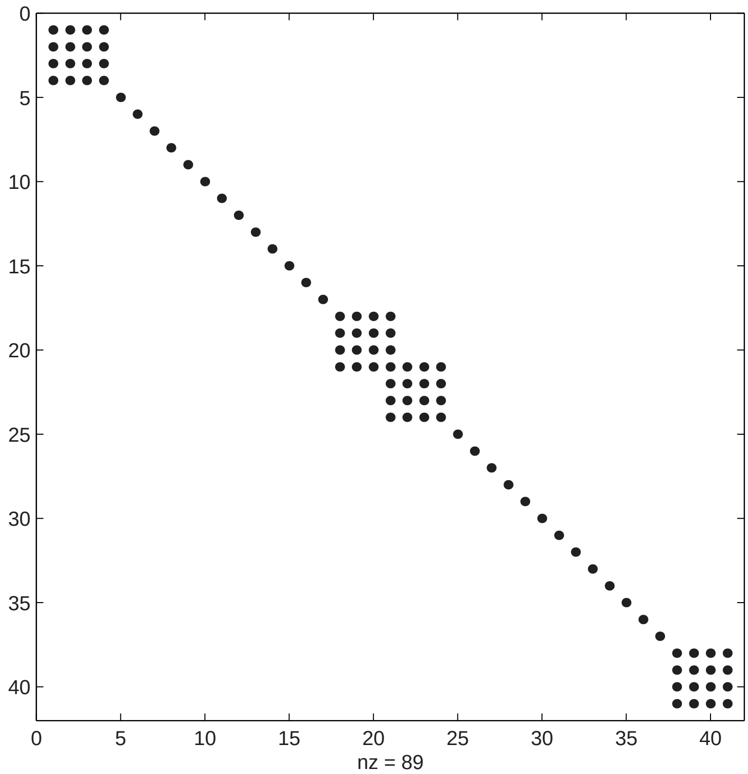

Figure 5: Lumped mass matrix for the impedance boundary condition in two media.

5 Error analysis

This section presents a reflection analysis of the errors including the boundaries associated with the approximations introduced in the last sections. Comparisons are made with the one-sided and centered approximations at the boundaries. It should be noted that for the Dirichlet and impedance boundary conditions, we consider an incoming wave from $+\infty$ as being reflected at $x = 0$ as shown in the diagram.

The Galerkin method, ie., FEM, can now be viewed as a difference method for u_j

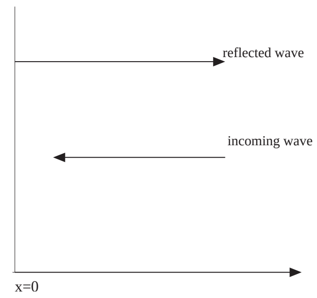

Figure 6: Reflection of a wave traveling to the left.

$$\ell(u_j) = \frac{1}{h^2}(a_3u_{j-3}+a_2u_{j-2}+a_1u_{j-1}+a_0u_j+a_1u_{j+1}+a_2u_{j+2}+a_3u_{j+3})+$$
$$k^2(b_3u_{j-3}+b_2u_{j-2}+b_1u_{j-1}+b_0u_j+b_1u_{j+1}+b_2u_{j+2}+b_3u_{j+3}) = 0 \quad (5.1)$$

Since the scheme is symmetric,

$$\ell(u_j) = c_3u_{j-3}+c_2u_{j-2}+c_1u_{j-1}+c_0u_j+c_1u_{j+1}+c_2u_{j+2}+c_3u_{j+3} = 0 \quad (5.2)$$

where

$$c_i = \frac{1}{h^2}a_i + k^2b_i$$

To do an error analysis for the scheme, we consider the finite difference formulation of the problem in order to apply the technique used for finite differences rather than for FEM.
The characteristic equation for (5.2) is

$$c_3\kappa^{-3} + c_2\kappa^{-2} + c_1\kappa^{-1} + c_0 + c_1\kappa + c_2\kappa^2 + c_3\kappa^3 = 0 \quad (5.3)$$

It can be shown easily that if κ is a solution of (5.1) then $\frac{1}{\kappa}$ is also a solution.
To solve this equation, let

$$\kappa_1 = e^{ikh+ir}$$

where κ_1 is the principal root, then one can write the equation as follows

$$c_0 + c_1(2cos(kh+r)) + c_2(2cos(2(kh+r))) + c_3(2cos(3(kh+r))) = 0$$

Put $s = kh$, expand in Taylor series and neglecting high powers of r yields

$$-2sr - \frac{-17}{6048}s^8 + \mathcal{O}(s^9r) = 0$$

which implies

$$r = \frac{-17}{12096}s^7 + \mathcal{O}(s^8)$$

and

$$\kappa_1 \approxeq e^{ikh(1-\frac{17}{12096}(kh)^7)}$$

Observe that

$$ir = \mathcal{O}(s^7).$$

Similarly for FDM, one can show that

$$ir = \mathcal{O}(s^5)$$

The spurious roots are simple roots. This implies that they can be found by setting the coefficients that correspond to the mass matrix equal to zero and from above it suffices to list only these

$$\kappa_2 = \frac{-1}{14} + \frac{3}{14}\sqrt{305} - \frac{-1}{14}\sqrt{2550 - 6\sqrt{305}} \approxeq 0.1388$$

$$\kappa_3 = \frac{-1}{14} + \frac{-3}{14}\sqrt{305} + \frac{1}{14}\sqrt{2550 + 6\sqrt{305}} \approxeq -0.1334$$

Now consider the incoming wave κ_1^{-n} where κ_1 is the principal root and suppose the boundary condition is of Dirichlet type, then the analytic solution on $x \geq 0$ is

$$u(x) = e^{-ikx} - e^{ikx} \tag{5.4}$$

and the numerical solution in terms of the principal root is

$$u_n = \kappa_1^{-n} - \kappa_1^n + e_n$$

which is equivalent to

$$u_n = (-1 + A_1)\kappa_1^n + A_2\kappa_2^n + A_3\kappa_3^n + \kappa_1^{-n};\ |\kappa_2| < 1,\ |\kappa_3| < 1 \tag{5.5}$$

The error is

$$u(x_n) - u_n = e_n + e^{-ikx_n} - k_1^{-n} - e^{ikx_n} + k_1^n$$

$$e_n = \begin{cases} A_1\kappa_1^n + A_2\kappa_2^n + A_3\kappa_3^n & , n \geq 1 \\ 0 & ,\text{n=0} \end{cases}$$

where e_n represents the error due to the boundary approximation. Then e_n satisfies the difference equation (5.1). Substituting into the difference equations at the boundary yields a linear system of equations in the unknowns

A_1, A_2 and A_3 while κ_1, κ_2 and κ_3 are the roots obtained above. Since $|\kappa_2| < 1$, $|\kappa_3| < 1$, we take $\kappa_2 = 0.1388$ and $\kappa_3 = -0.1334$. This linear system has the following form

$$\frac{1}{h^2}Cx = b \tag{5.6}$$

where $C = C_1 + \mathcal{O}(h) + \mathcal{O}(h^2)$ and

$$C_1 = \begin{pmatrix} -1.467 & 0.444 & -0.395 \\ 0.299 & -0.284 & 0.197 \\ 0.044 & 0.041 & 0.0006 \end{pmatrix}$$

$$x = \begin{pmatrix} A_1 \\ A_2 \\ A_3 \end{pmatrix}$$

$$b = \begin{pmatrix} c_1 h^3 \\ c_2 h^3 \\ c_3 h^3 \end{pmatrix}$$

with c_1, c_2 and c_3 are the constants obtained by Taylor series expansion for the first three rows. These are $c_1 = 79/72$, $c_2 = 173/90$ and $c_3 = 1087/360$. In this linear system of equations it suffices to show that the determinant of the matrix of the coefficient C is nonzero for all sufficiently small h. In our case we have shown that det(C) is different from zero. Hence we conclude that the order of accuracy is of $\mathcal{O}(h^5)$.

We have obtained the same order using a centered scheme at the boundary. However it is a known fact that different methods of the same order can have different errors, they are distinguished by the error constants. As a comparison for the same problem, using a centered scheme where α is 0 and 0.5, (see, fig3) we got C_1 and b to be respectively

$$C_1 = \begin{pmatrix} -1/45 & -0.0028 & -0.0026 & 0.0019 \\ 1/60 & -1.03 & 0.297 & -0.270 \\ -7/360 & -0.014 & -0.179 & 0.107 \\ 0 & 1.06 & 0.0204 & 0.0245 \end{pmatrix}$$

$$b = \begin{pmatrix} \frac{-7}{360} h^3 \\ \frac{353}{360} h^3 \\ 2h^3 \\ 3h^3 \end{pmatrix}$$

and

$$C_1 = \begin{pmatrix} -0.001 & 0.0009 & -0.0014 & 0.0012 \\ 0.009 & -2.10 & 0.439 & -0.418 \\ 0.006 & -0.021 & -0.175 & 0.104 \\ -0.002 & 0.019 & 0.017 & 0.022 \end{pmatrix}$$

$$b = \begin{pmatrix} -0.00517h^3 \\ .5h^3 \\ 1.4h^3 \\ 2.5h^3 \end{pmatrix}$$

Note that in these two cases

$$e_n = \begin{cases} A_1\kappa_1^n + A_2\kappa_2^n + A_3\kappa_3^n & ,n \geq 1 \\ 0 & ,\text{n=0} \\ A_{-1} & ,\text{n=-1} \end{cases}$$

Hence,

$$x = \begin{pmatrix} A_{-1} \\ A_1 \\ A_2 \\ A_3 \end{pmatrix}$$

Solving the three different systems of equations, the unknowns were found to be, for the one-sided scheme at the boundary

$$x = \begin{pmatrix} -13.9h^5 \\ 56.1h^5 \\ 112.2h^5 \end{pmatrix}$$

for the centered scheme at the boundary, ie., for $\alpha = 0$

$$x = \begin{pmatrix} -1.19h^5 \\ 7.68h^5 \\ -91.36h^5 \\ -133.7h^5 \end{pmatrix}$$

while for $\alpha = 0.5$

$$x = \begin{pmatrix} 61.4h^5 \\ -11.1h^5 \\ 53.3h^5 \\ 111h^5 \end{pmatrix}$$

We see from the values of the unknowns A_i's, in particular the value of A_1, is smaller in the centered schemes at the boundary rather than in the one-sided schemes at the boundary. It should be noted that the reason we compared the values of A_1 is that it is the constant term of the non-decaying κ_1. Hence we conclude that centered schemes at the boundary are better. In a similar fashion applying the techniques discussed above we show for the other boundary conditions (Neumann and impedance) and also for the FDM schemes.

6 Numerical Examples

In this section some of the numerical experiments that have been performed are described. Consider

$$\frac{\partial^2 u}{\partial x^2} + k^2 u = (k^2 - \pi^2) sin(\pi x), \ 0 \le x \le 1 \quad (6.1)$$

$$u(0) = 0 \quad (6.2)$$

$$u(1) = 0 \quad (6.3)$$

The exact solution is

$$u(x) = sin(\pi x), \ 0 \le x \le 1 \quad (6.4)$$

The FEM and FDM (lumped mass) solutions are obtained. Table 11 shows a grid refinement study for the problem.

h	FEM (l^∞)	Lumped (l^∞)	rate(FEM)	rate(Lumped)
0.1	1.0254×10^{-4}	3.3300×10^{-4}	–	–
0.05	3.4014×10^{-6}	2.0667×10^{-5}	4.91	4.00
0.025	1.0784×10^{-7}	1.2927×10^{-6}	5.00	4.00

Table 11: Dirichlet boundary condition.

The second numerical example is the Neumann boundary condition.

$$\frac{\partial^2 u}{\partial x^2} + k^2 u = (k^2 - \pi^2) cos(\pi x), \ 0 \le x \le 1 \quad (6.5)$$

$$\frac{du(0)}{dx} = 0 \quad (6.6)$$

$$\frac{du(1)}{dx} = 0 \quad (6.7)$$

Here, the exact solution is

$$u(x) = cos(\pi x),\ 0 \le x \le 1 \tag{6.8}$$

The numerical solutions of the FEM and FDM are obtained, and a grid refinement study for both follows in the following table.
Furthermore, the numerical solution for the impedance boundary condition

h	FEM (l^{∞})	Lumped (l^{∞})	rate(FEM)	rate(Lumped)
0.1	1.8711×10^{-4}	.0020	–	–
0.05	1.4604×10^{-5}	1.3188×10^{-4}	3.68	3.94
0.025	1.0850×10^{-6}	8.1774×10^{-6}	3.76	4.00

Table 12: Neumann boundary condition

$$\frac{du}{dx} + iku = 2ike^{ikx},\ x = 0 \tag{6.9}$$

$$\frac{du}{dx} - iku = 0, x = 1 \tag{6.10}$$

is obtained, and table 13 gives the convergence rates of both the FEM and FDM (lumped). Note that the analytic solution of this problem is

$$u(x) = e^{ikx} \tag{6.11}$$

h	FEM (l^{∞})	Lumped (l^{∞})	rate(FEM)	rate(Lumped)
0.01	1.4402×10^{-5}	2.7715×10^{-4}	–	–
0.005	9.0813×10^{-7}	1.8867×10^{-5}	3.99	3.88
0.0025	5.6883×10^{-8}	1.2058×10^{-6}	4.00	3.97

Table 13: Impedance boundary condition.

As an illustration, the following graphs were taken for the (6.9) and (6.10), with impedance boundary conditions for both FEM and FDM (Lumped) schemes.

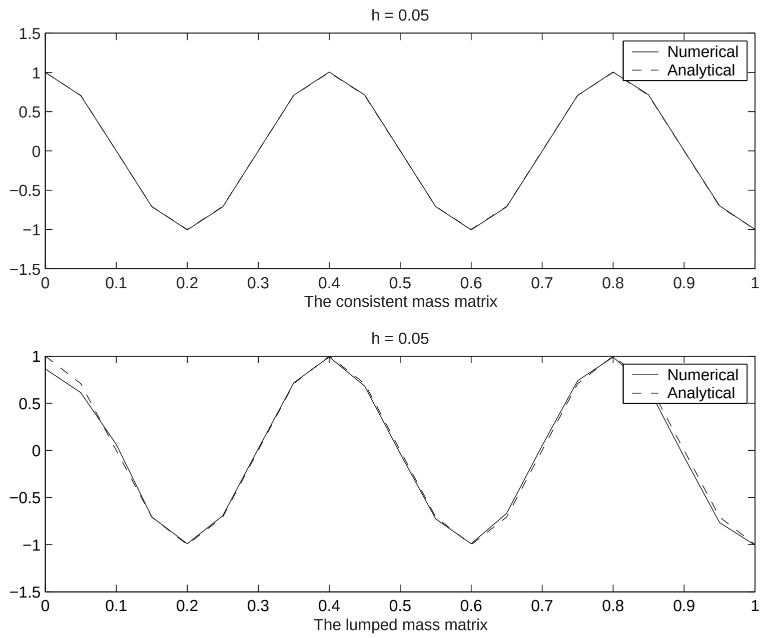

Figure 7: Graphs for FEM(top) and for FDM with step size $h = 0.05$

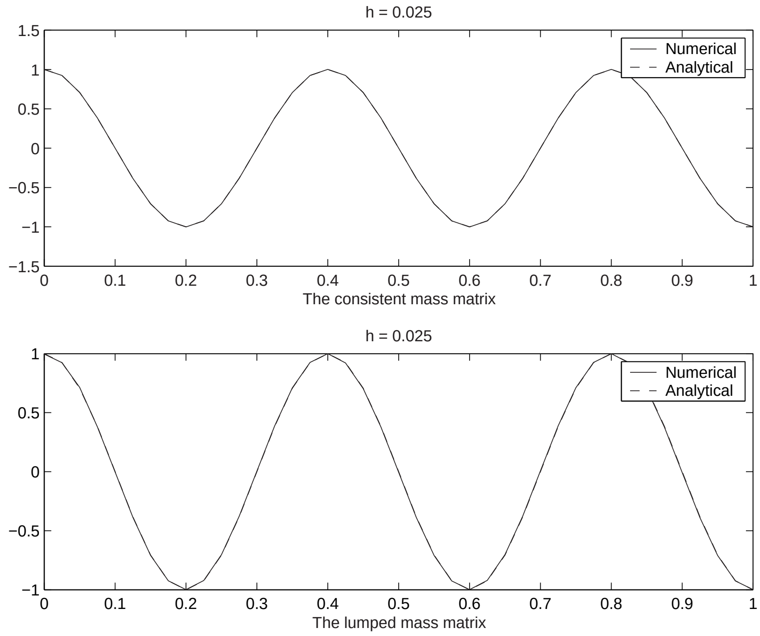

Figure 8: Graphs for FEM(top) and for FDM with step size $h = 0.025$

Finally, for the two media case given in (2.10) with

$$\frac{du}{dx} + ik_1 u = 2ik_1 e^{ik_1 x}, x = -1 \tag{6.12}$$

$$\frac{du}{dx} - ik_2 u = 0, x = 1 \tag{6.13}$$

We have tested for different step sizes h_1 and h_2 and different densities. For equal step sizes, table(14) shows the rate of convergence.

$h = h_1 = h_2$	FEM (l^∞)	Lumped (l^∞)	rate(FEM)	rate(Lumped)
0.01	1.4419×10^{-5}	2.5×10^{-3}	–	–
0.005	9.0825×10^{-7}	1.4296×10^{-4}	3.99	4.00
0.0025	5.6883×10^{-8}	8.6991×10^{-6}	4.00	4.00

Table 14: Impedance boundary condition in two media

In addition, the following graphs illustrate the two methods, FEM and FDM for the two media problem with different step sizes.

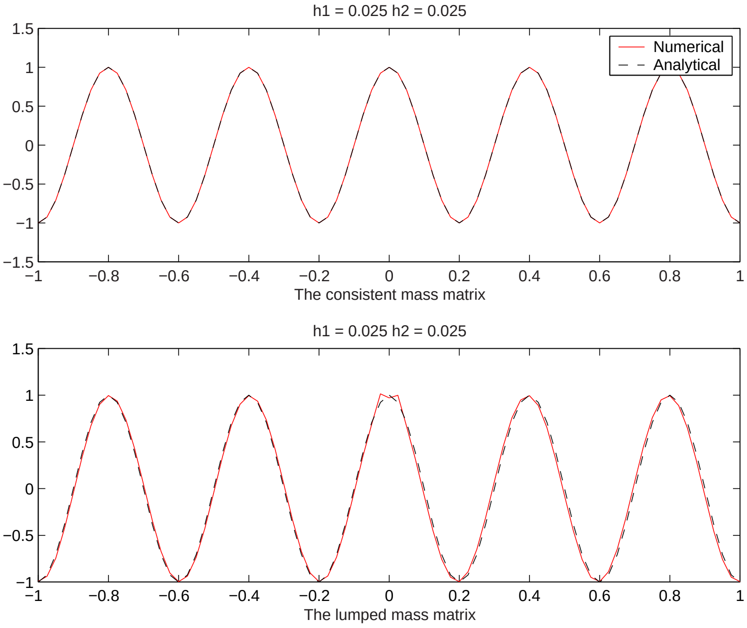

Figure 9: Graphs of FEM(top) and FDM with step size $h = 0.025$.

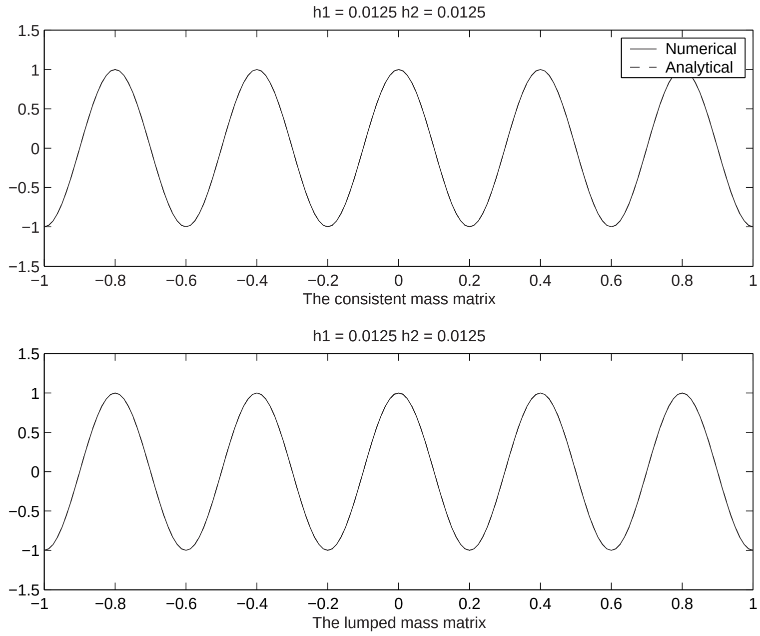

Figure 10: Graphs of FEM(top) and FDM with step size $h = 0.0125$.

Observe, the lumped scheme(FDM) needs finer step size to reach asymptotic range of accuracy.

7 Time Dependent Problems

Although, FEM is usually thought of as a method of discretization in space, it can be used in time as well. However, here we use the method of lines [4]. It allows the space discretization to be handled separately. Consequently, for the wave equation (1.1), we have used finite difference approximations for the time derivative terms obtained by Taylor series combined with the FEM in space .

At first we consider the wave equation

$$\frac{1}{c^2}\frac{\partial^2 u}{\partial t^2} = \frac{\partial^2 u}{\partial x^2},\ 0 \leq x \leq 1\ , t \geq 0 \tag{7.1}$$

$$u(x,0) = f(x) \tag{7.2}$$

$$\frac{\partial}{\partial t}u(x,0) = g(x) \tag{7.3}$$

with Dirichlet boundary conditions

$$u(0,t) = u(1,t) = 0 \tag{7.4}$$

Discretizing the spatial part of the equation by Galerkin method leads to a system of ordinary differential equations in time.

$$M\frac{\partial^2 u}{\partial t^2} = Su \tag{7.5}$$

We now look at the time discretization of the system of ordinary differential equations (7.5) by FDM.

We approximate the time derivative by a centered fourth order accurate finite difference formula as follows.

$$\frac{\partial^2 u}{\partial t^2} = \frac{u^{n+1} - 2u^n + u^{n-1}}{(\triangle t)^2} - \frac{(\triangle t)^2}{12}\frac{\partial^4 u}{\partial t^4} + \mathcal{O}((\triangle t)^4) \tag{7.6}$$

From (7.5)

$$\frac{\partial^2 u}{\partial t^2} = M^{-1}Su$$

which implies

$$\frac{\partial^4 u}{\partial t^4} = M^{-1}S\frac{\partial^2 u}{\partial t^2}$$

ie.,

$$\frac{\partial^4 u}{\partial t^4} = M^{-1}S(M^{-1}Su)$$

substituting (7.6) into (7.5), we obtain

$$u^{n+1} = 2u^n - u^{n-1} + (\triangle t)^2 M^{-1} S(u^n + \frac{(\triangle t)^2}{12} M^{-1} S u^n) \qquad (7.7)$$

where M and S are the mass and stiffness matrices respectively. In addition to the Dirichlet boundary condition, the other types of boundary conditions, such as, the Neumann boundary condition

$$\frac{\partial u(0,t)}{\partial x} = \frac{\partial u(1,t)}{\partial x} = 0 \qquad (7.8)$$

and the impedance boundary condition

$$\frac{\partial u}{\partial x} - \frac{1}{c}\frac{\partial u}{\partial t} = -\frac{2}{c}\frac{\partial f(t)}{\partial t} \qquad (7.9)$$

were also applied.
we have taken as first step the following boundary conditions

$$\frac{\partial u}{\partial x}(0,t) = \alpha u(0,t) \qquad (7.10)$$

$$u(1,t) = 0 \qquad (7.11)$$

Exact solutions may be given by

$$u(x,t) = sin(\beta(x-1))sin\beta t \qquad (7.12)$$

and

$$\alpha = \frac{\beta cos\beta}{-sin\beta} \qquad (7.13)$$

For instance when $\beta = 2$ we have the following graph

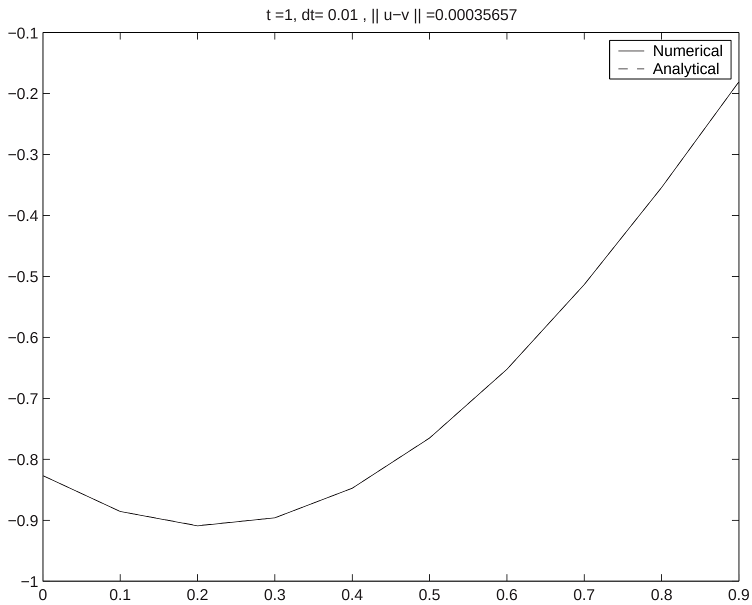

Figure 11: FEM graph for the boundary conditions given in (7.10) and (7.11).

Finally the equation is also solved in two media. The problem is posed as follows. Let u_1 and u_2 be the solutions of the equation in media I and II respectively, then the equations are

$$\frac{1}{c_1^2}\frac{\partial^2 u_1}{\partial t^2} = \frac{\partial^2 u_1}{\partial x^2}, \ -1 \leq x \leq 0 \ , t \geq 0 \tag{7.14}$$

$$\frac{\partial u_1}{\partial x} - \frac{1}{c_1}\frac{\partial u_1}{\partial t} = -\frac{2}{c_1}\frac{\partial f(t)}{\partial t}, \ x = -1 \tag{7.15}$$

and

$$\frac{1}{c_2^2}\frac{\partial^2 u_2}{\partial t^2} = \frac{\partial^2 u_2}{\partial x^2}, \ 0 \leq x \leq 1 \ , t \geq 0 \tag{7.16}$$

$$\frac{\partial u_2}{\partial x} + \frac{1}{c_2}\frac{\partial u_2}{\partial t} = 0, \ x = 1 \tag{7.17}$$

The complete solution u_1 contains two arbitrary, but twice differentiable, functions

$$u_1(x,t) = f(x - c_1 t) + g(x + c_1 t), \tag{7.18}$$

while

$$u_2(x,t) = h(x - c_2 t) \tag{7.19}$$

The second solution (7.19) is a wave traveling to the right, while a reflected wave traveling to the left is not allowed, according to the boundary condition (7.17).
We use

$$f(x - c_1 t) = e^{-\alpha(x - c_1 t + \gamma)^2},$$

$$g(x + c_1 t) = \frac{c_2\rho_2 - c_1\rho_1}{c_1\rho_1 - c_2\rho_2} e^{-\alpha(-x - c_1 t + \gamma)^2}$$

and

$$h(x - c_2 t) = \frac{2c_2\rho_2}{c_1\rho_1 + c_2\rho_2} e^{-\alpha((x - c_2)t\frac{c_1}{c_2} + \gamma)^2}$$

which are obtained by making use of the continuity equations (2.8) and (2.9) at the interface between the two media. Furthermore, numerically, it is also not easy to implement as the boundary condition contains a derivative in time. It is formulated as

$$\frac{1}{c^2} M \frac{\partial^2 u}{\partial t^2} + A \frac{\partial u}{\partial t} + Su = F(t) \tag{7.20}$$

where M and S are the mass and stiffness matrices respectively and

$$A = \begin{pmatrix} 1 & 0 & \dots & 0 \\ 0 & 0 & \dots & 0 \\ \vdots & \vdots & & \vdots \\ 0 & 0 & \dots & 1 \end{pmatrix}$$

and

$$F(t) = \begin{pmatrix} \frac{2}{c_1} \frac{df(0,t)}{dt} \\ 0 \\ 0 \\ \vdots \\ 0 \\ 0 \end{pmatrix}$$

Substituting the fourth order finite difference in time for $\frac{\partial^2 u}{\partial t^2}$ and central difference in time for $\frac{\partial u}{\partial t}$, the following is obtained.

$$Q_1 u^{n+1} = Q_2 u^n + Q_3 u^{n-1} + F \tag{7.21}$$

where

$$Q_1 = \frac{M}{(\triangle t)^2} + \frac{AM^{-1}A}{12} - \frac{\triangle t}{24}AM^{-1}S - \frac{S}{12} + \frac{A}{2\triangle t}$$

$$Q_2 = \frac{2M}{(\triangle t)^2} - \frac{AM^{-1}A}{6} - \frac{S}{6} - \frac{M^{-1}A}{3}$$

$$Q_3 = \frac{M}{(\triangle t)^2} + \frac{AM^{-1}A}{12} + \frac{\triangle t}{24}AM^{-1}S - \frac{S}{12} + \frac{A}{2\triangle t}$$

and

$$F = \frac{(\triangle t)^2}{12}AM^{-1}\frac{dF}{dt} - \frac{(\triangle t)^2}{12}\frac{d^2F}{dt^2} - \frac{(\triangle t)^2}{6}M^{-1}\frac{dF}{dt}$$

To see how the finite difference obtained by lumping performs with time dependent problems comparing to steady state problems such as the Helmholtz equation discussed earlier, we consider the following numerical examples

$$\frac{1}{c^2}\frac{\partial^2 u}{\partial t^2} = \frac{\partial^2 u}{\partial x^2}, \; 0 \le x \le 1 \;, t \ge 0 \tag{7.22}$$

$$u(x,0) = sin\pi x \tag{7.23}$$

$$\frac{\partial}{\partial t}u(x,0) = 0 \tag{7.24}$$

with Dirichlet boundary conditions

$$u(0,t) = u(1,t) = 0 \tag{7.25}$$

h	$\triangle t$	FEM (l^∞)	FDM (l^∞)	rate(FEM)	rate(FDM)
0.01	.001	8.7743×10^{-10}	1.7955×10^{-9}	–	–
0.005	.001	2.8935×10^{-11}	5.5023×10^{-11}	4.92	5.02

Table 15: Rate of convergence for Dirichlet boundary conditions

With impedance boundary condition

$$\frac{\partial u}{\partial x}(0,t) = \alpha u(0,t) \tag{7.26}$$

$$u(1,t) = 0 \tag{7.27}$$

with α given in (7.13).

h	$\triangle t$	FEM (l^∞)	FDM (l^∞)	rate(FEM)	rate(FDM)
0.01	.001	4.025×10^{-5}	3.565×10^{-4}	–	–
0.005	.001	2.7015×10^{-6}	2.2430×10^{-5}	3.89	3.99

Table 16: Rate of convergence for the impedance boundary conditions

As a third example

$$\frac{1}{c^2}\frac{\partial^2 u}{\partial t^2} = \frac{\partial^2 u}{\partial x^2}, \; 0 \leq x \leq 1 \; , t \geq 0 \tag{7.28}$$

$$\frac{\partial u}{\partial x} - \frac{1}{c}\frac{\partial u}{\partial t} = -\frac{2}{c}\frac{\partial f(t)}{\partial t}, \; x = 0 \tag{7.29}$$

$$\frac{\partial u}{\partial x} + \frac{1}{c}\frac{\partial u}{\partial t} = 0, \; x = 1 \tag{7.30}$$

Observe that we are using a symmetric positive definite matrix for FDM as remarked in section 2. The following table shows the rate of convergence.

h	$\triangle t$	FEM (l^∞)	FDM (l^∞)	rate(FEM)	rate(FDM)
0.01	.001	8.4705×10^{-5}	0.0188	–	–
0.005	.001	4.5987×10^{-6}	6.47×10^{-4}	3.75	4.85

Table 17: Rate of convergence for the impedance inflow boundary conditions.

At last, for the two media problem (7.13-7.16) taking $\alpha = 200$ and $\rho = 1.3$, the rate of convergence using a fourth order finite difference in time is given below

$h = h_1 = h_2$	$\triangle t$	FEM (l^∞)	FDM (l^∞)	rate(FEM)	rate(FDM)
0.01	.001	8.4705×10^{-5}	0.0188	–	–
0.005	.001	4.5987×10^{-6}	6.47×10^{-4}	3.75	4.85

Table 18: Rate of convergence for the impedance boundary condition in two media.

The following graph illustrates this last example

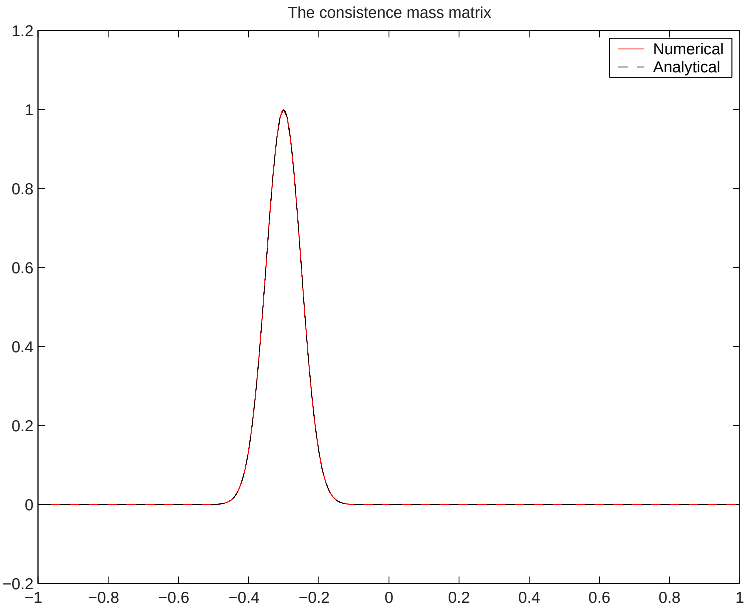

Figure 12: FEM and FDM in two media using fourth order finite difference in time.

8 CONCLUSION

In this paper FEM and FDM solutions of the Helmholtz equation in one dimension with different boundary conditions for the one medium and two media cases have been considered. The PDE is discretized by the Galerkin method. The main objective of the paper is to develop high order symmetric finite difference approximations that will be employed for the wave equation. FEM constructed for the Helmholtz equation have been shown to perform well for the Dirichlet boundary condition compared to FDM. The analysis and the numerical experiments described in the paper show that the error of FEM is $\mathcal{O}(h^5)$ while the error of FDM(lumped) is $\mathcal{O}(h^4)$. In addition it is observed that the error of FEM in the interior is of $\mathcal{O}(h^6)$ for the Helmholtz equation while the error of FDM is only $\mathcal{O}(h^4)$. This means that for this particular equation FEM is superior with regard to the rate of convergence. Hence it is not significant to lump the mass matrix in order to obtain FDM for the Dirichlet boundary condition despite the latter is symmetric. In other words if one is interested in the order of accuracy of a scheme for the wave equation, FEM should be used. Moreover, although FEM and FDM both have the same order of accuracy in the Neumann boundary condition case the latter yields bigger error coefficient than the former. Hence, we infer that FEM is better in frequency domain problems. Also as it is explained in the paper for the impedance boundary condition where we have time derivatives in the expression of the boundary, it is not possible to have diagonal lumped mass matrix(FDM) that retains the order of accuracy to implement it in the time domain. It is done by a positive definite symmetric matrix rather than a diagonal matrix which affects the cost when we implement it in higher dimensions.

The other comparison we have made is among the one-sided scheme at the boundary and centered scheme at the boundary, and it is shown that the latter works better which coincides with the known fact from the theory of finite differences [5].

For time dependent problems, FEM with Dirichlet boundary condition retains the super-convergence and FDM yields the desired accuracy. However for the Neumann boundary condition both acquired the same order of accuracy showing FDM which is symmetric (being diagonal matrix) attains high order accuracy as desired. For the third type of boundary condition, the impedance, imposing time-dependent boundary condition, FDM is symmetric and positive definite and the expected rate of convergence is obtained but the scheme needs finer space step size to reach asymptotic range of accuracy.

Moreover, the advantage of the FDM is its added stability condition. It was found by applying von-Neumann analysis, for the Cauchy problem that the stability condition is $c\triangle t < 1.7h$ for FDM, whereas $c\triangle t < h$ for FEM. In both cases c was taken to be 1. Note that since we are considering boundary value problem the CFL condition is slightly diferent from the Cauchy problem. This implies that we have achieved a consistent difference equation with a typical Courant condition for numerical stability. Hence for time dependent problems and for the wave equation, it is of great importance to lump the mass matrix thereby obtaining FDM scheme.

REFERENCES

[1] B.Swartz and B.Wendroff. The relative efficiency of finite difference and finite element methods I: Hyperbolic problems and splines, SIAM J. Numer. ANAL.,11 (1974), pp. 979-993.

[2] P.Olsson, D. Gottlieb, B. Gustafsson, B. Strand, On the super-convergence of Galerkin methods for Hyperbolic IBVP, SIAM J.Numer. ANAL., 33(1996), pp. 1778-1796.

[3] STRANG,G and Fix,G. An analysis of the finite element method. 1973, Prentice-Hall,Inc.,Englewood Cliffs, N.J.

[4] B.Gustafson, H.-O.Kreiss, and J.Oliger. Time Dependent problems and Difference Methods. Wiley and Sons,1995.

[5] H.-O.KREISS, Difference approximations for boundary and eigenvalue problems for ordinary differential equations, Math.Comp., 26(1972), pp.605-624.

[6] V.THOMÉE AND B.WENDROFF, Convergence estimates for Galerkin methods for variable coefficient initial value problems, SIAM J.Numer.Anal., 11(1974), pp.1059-1068.

[7] B.SWARTZ AND B.WENDROFF, Generalized finite-difference schemes, Math.Comp.,23(1969), pp.37-49.

[8] H.O. Kreiss and J. Oliger. Comparison of accurate methods for the integration of hyperbolic equations. Tellius,24(1972),pp.199-215.

[9] B.GUSTAFSSON, The convergence rate for difference approximations to general mixed initial boundary value problem, SIAM J.Numer Anal, 18(1981), pp. 179-190

[10] V.THOMÉE, Spline approximation and difference scheme for the heat equation, The Mathematical Foundation of the Finite Element Method with Application to partial Differential Equations, A.K. Aziz,ed., Academic Press, New York. 1972

[11] M.H.Carpenter, D.Gottlieb, and S.Abarbanel. Time-stable boundary conditions for finite-difference schemes solving hyperbolic systems: Methodology and application to high-order compact schemes. J. Comput. Phys., 111(2):220-236, Apr. 1994

[12] Douglas J. Riley. Transient Finite-Elements for Computational Electromagnetics: Hybridization with Finite Differences, Modeling Thin Wires and Thin slots, and Parallel processing. applied Computational Electromagnetics Society(ACES) Symposium, Monterey, California, March 2001

Recent Licentiate theses from the Department of Information Technology

2001-004 Bengt Eliasson: *Numerical Simulation of Kinetic Effects in Ionospheric Plasma*

2001-005 Per Carlsson: *Market and Resource Allocation Algorithms with Application to Energy Control*

2001-006 Bengt Göransson: *Usability Design: A Framework for Designing Usable Interactive Systems in Practice*

2001-007 Hans Norlander: *Parameterization of State Feedback Gains for Pole Assignment*

2001-008 Markus Bylund: *Personal Service Environments — Openness and User Control in User-Service Interaction*

2001-009 Johan Bengtsson: *Efficient Symbolic State Exploration of Timed Systems: Theory and Implementation*

2001-010 Johan Edlund: *A Parallel, Iterative Method of Moments and Physical Optics Hybrid Solver for Arbitrary Surfaces*

2001-011 Pär Samuelsson: *Modelling and control of activated sludge processes with nitrogen removal*

2001-012 Per Åhgren: *Teleconferencing, System Identification and Array Processing*

2001-013 Alexandre David: *Practical Verification of Real-time Systems*

2001-014 Abraham Zemui: *Fourth Order Symmetric Finite Difference Schemes for the Wave Equation*

UPPSALA
UNIVERSITY

Department of Information Technology, Uppsala University, Sweden